Angle-tuned, evanescently-decoupled reflector for high-efficiency red light-emitting diode

Sun-Kyung Kim,[1,*] Hyun Kyong Cho,[1] Kyung Keun Park,[1] Junho Jang,[1] Jeong Soo Lee,[1] Kyung Wook Park,[2] Youngho Park,[2] Ju-Young Kim,[3] and Yong-Hee Lee[3]

[1]LED R&D Lab, LG Electronics Institute of Technology, Seoul 137-724, Korea
[2] EPIPLUS CO., LTD., Gwangju 500-460, Korea
[3]Department of Physics, Korea Advanced Institute of Science and Technology, Taejon 305-701, Korea
jclub@kaist.ac.kr

Abstract: We propose and demonstrate evanescently-decoupled, solid-angle-optimized distributed Bragg reflectors (DBRs) for AlGaInP light-emitting diodes (LEDs). The thickness of each DBR layer is tuned to the wavelength slightly longer than the emission peak of the active medium in order to maximize the radiated power integrated over the top surface. In addition, to increase the horizontal radiation through the side facets, the glancing-angle reflectivity at the AlInP/AlAs interface is improved by employing an AlAs layer thicker than the attenuation length of the evanescent field. With the improved DBR, the integrated output power of AlGaInP LEDs is enhanced by a factor of 1.9 in comparison to those of LEDs with conventional DBRs. Additional 1.25-fold enhancement is observed by incorporating an square-lattice hole array (a=1200nm) into the top GaP surface by a conventional photolithography.

OCIS codes: (050.5298) Photonic crystals (230.1480) Bragg reflectors (230.3670) Light-emitting diodes.

References and links

1. A. A. Efremov, N. I. Bochkareva, R. I. Gorbunov, D. A. Larinovich, Yu. T. Rebane, D. V. Tarkhin, and Yu. G. Shreter, "Effect of the joule heating on the quantum efficiency and choice of thermal conditions for high-power blue InGaN/GaN LEDs," Semiconductors **40**, 605-610 (2006).
2. J. J. Wierer, D. A. Steigerwald, M. R. Krames, J. J. O'Shea, M. J. Ludowise, G. Christenson, Y.-C. Shen, C. Lowery, P. S. Martin, S. Subramanya, W. Götz, N. F. Gardner, R. S. Kern, and S. A. Stockman, "High-power AlGaInN flip-chip light-emitting diodes," Appl. Phys. Lett. **78**, 3379-3381 (2001).
3. W. S. Wong, T. Sands, N. W. Cheung, M. Kneissl, D. P. Bour, P. Mei, L. T. Romano, and N. M. Johnson, "Fabrication of thin-film InGaN light-emitting diode membranes by laser lift-off," Appl. Phys. Lett. **75**, 1360-1362 (1999).
4. A. David, T. Fujii, B. Moran, S. Nakamura, S. P. DenBaars, C. Weisbuch, and H. Benisty, "Photonic crystal laser lift-off GaN light-emitting diodes," Appl. Phys. Lett. **88**, 133514 (2006).
5. Th. Gessmann and E. F. Schubert, "High-efficiency AlGaInP light-emitting diodes for solid-state lighting applications," J. Appl. Phys. **95**, 2203-2216 (2004).
6. J. Xu, H. Fang, and Z. Lin, "Expanding high-reflection range in a dielectric multilayer reflector by disorder and inhomogenity," J. Phys. D: Appl. Phys. **34**, 445-449 (2001).
7. S. Chiou, C. Lee, C. Huang, and C. Chen, "Wide angle distributed Bragg reflectors for 590 nm amber AlGaInP light-emitting diodes," J. Appl. Phys. **87**, 2052-2054 (2000).
8. J. –Q. Xi, M. Ojha, J. L. Plawsky, W. N. Gill, J. K. Kim, and E. F. Schubert, "Internal high-reflectivity omni-directional reflectors," Appl. Phys. Lett. **87**, 031111 (2005).
9. T. Fujii, Y. Gao, R. Sharma, E. L. Hu, S. P. Denbaars, and S. Nakamura, "Increase in the extraction efficiency of GaN-based light-emitting diodes via surface roughening," Appl. Phys. Lett. **84**, 855-857 (2004).
10. S. Fan, P. R. Villeneuve, J. D. Joannopoulos, and E. F. Schubert, "High Extraction Efficiency of Spontaneous Emission from Slabs of Photonic Crystals," Phys. Rev. Lett. **78**, 3294-3297 (1997).
11. H. K. Cho, J. Jang, J. H.Choi, J. Choi, J. Kim, J. J. Lee, B. Lee, Y. H. Choe, K. D. Lee, S. H. Kim, K. Lee, S. K. Kim, and Y. H. Lee, "Light extraction enhancement from nano-imprinted photonic crystal GaN-based blue light-emitting diodes," Optics Express **14**, 8454 (2006).

#92654 - $15.00 USD Received 11 Feb 2008; revised 9 Apr 2008; accepted 9 Apr 2008; published 14 Apr 2008

12. M. R. Krames, M. O. -Holcomb, G. E. Höfler, C. C. -Coman, E. I. Chen, I.-H. Tan, P. Grillot, N. F. Gardner, H. C. Chui, J.-W. Huang, S. A. Stockman, F. A. Kish, M. G. Craford, T. S. Tan, C. P. Kocot, M. Hueschen, J. Posselt, B. Loh, G. Sasser, and D. Collins, "High-power truncated- pyramid (AlGa)InP/GaP light-emitting diodes exhibiting >50% external quantum efficiency," Appl. Phys. Lett. **75**, 2365-2367 (1999).
13. H. Ichikawa and T. Baba, "Efficiency enhancement in a light-emitting diode with a two-dimensional surface grating photonic crystal," Appl. Phys. Lett. **84**, 457-459 (2004).
14. T. Kim, P. O. Leisher, A. J. Danner, R. Wirth, K. Streubel, and K. D. Choquette, "Photonic crystal structure effect on the enhancement in the external quantum efficiency of a red LED," IEEE Photon. Technol. Lett. **17**, 1876-1878 (2006).
15. A. David, T. Fujii, R. Sharma, K. McGroddy, S. Nakamura, S. P. DenBaars, E. L. Hu, and C. Weisbuch, "Photonic-crystal GaN light-emitting diodes with tailored guided mode distribution," Appl. Phys. Lett. **88**, 061124 (2006).

1. Introduction

Light-emitting diodes (LEDs) have been widely recognized as energy-saving and environment-friendly light sources. Thanks to the rapid improvement of internal- and extraction efficiencies, high-brightness LEDs become more popular and are steadily making inroads into the domains of classical incandescent or fluorescent lamps. Especially, once the overall efficiency of the white LEDs exceeds ~100 lm/W, they are expected to be deployed for mundane applications such as interior illuminations, back light units, color therapy and so on. Towards this end, the enhancement of the efficiency still remains an important on-going issue.

Several technical problems need to be addressed for high-efficiency LEDs. First of all, defect-free epitaxial growth is important to improve the internal quantum efficiency. Up to date, the epitaxial growth conditions have been stabilized for most existing semiconductor materials. Thus, the reliability of the device becomes as important as the output efficiency. Second, the issue of heat generation and thermal dissipation becomes more critical than ever for commercially viable LED devices. The internal quantum efficiency tends to deteriorate with the increase of the device temperature [1]. Therefore, particularly for high-current, high-power applications, it is crucial to keep the overall efficiency from degradation. For instance, metal-bonding substrates or packages made of thermally conductive materials have been employed [2-4]. Lastly, the efforts toward better light extraction should be addressed. This part still has some room for improvement. The light extraction enhancement relies on both high-reflectivity bottom mirrors [5-8] and efficient light extraction structures [9-11]. Major fraction of photons generated inside an LED undergoes multiple reflections from the internal mirror and unavoidable absorption losses accumulate upon every reflection. Therefore, an efficient outcoupling structure is needed to extract confined photons before they are absorbed.

In this letter, we focus on the enhancement of the extraction from AlGaInP red (λ_c=625 nm) LEDs. Our AlGaInP LEDs employ AlAs/AlGaAs distributed Bragg reflectors (DBRs) as a bottom mirror. The thickness of each DBR layer is slightly modified from the conventional quarter-wave (λ/4n) DBR, maintaining the equal number of pairs. The modified DBR shows higher reflectivity over an extended range of angle. For comparison purposes, we prepare two LED structures with conventional and modified DBRs. In addition, we incorporate square-lattice periodic holes (a=1200 nm) into the top p-doped GaP surface to further increase the output power. The periodic pattern is prepared by a conventional photolithography (g-line) that is suitable for low-cost mass production.

2. Conventional quarter-wave DBRs

The LED with a conventional DBR, made for comparison purposes, consists of 12-pairs of AlAs- (n_L=3.13) and $Al_{0.5}Ga_{0.5}As$ (n_H=3.55) layer (Fig. 1(a)). The thickness of each DBR layer is quarter-wave (λ/4n) at 625 nm. The Al fraction of 0.5 in the AlGaAs layer is selected to stay away from the absorption band. The conventional DBR mirror mainly reflects the radiation propagating vertically (Fig. 1(b)). At the center wavelength (λ_c=625nm) of the AlGaInP LED, the angular reflectance is plotted as shown in Fig. 2(a). Here, the DBR is

#92654 - $15.00 USD Received 11 Feb 2008; revised 9 Apr 2008; accepted 9 Apr 2008; published 14 Apr 2008

designed for the normally-incident waves and the resultant reflectivity is >80%. However, note that the reflectivity becomes negligible when the incident angle is larger than the cut-off angle (~15°). The cut-off angle is determined by the index contrast of AlAs and AlGaAs and the number of quarter-wave pairs.

There are two allowed radiation paths in this structure: the vertical path through the top surface and the horizontal path through four side facets. If emitted photons fall in either of two gray regions shown in Fig. 2(a), they can escape out of the LED. Therefore, the total flux within these two angular ranges is of special importance connected to the output power measured by an integration sphere.

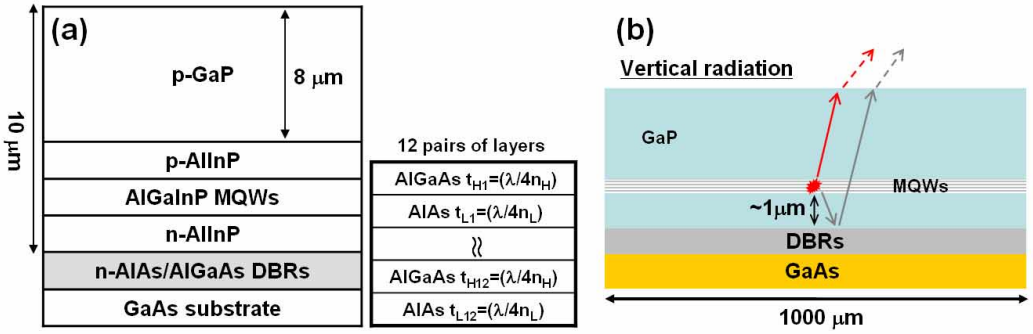

Fig. 1. (a) Detailed epitaxial structure of the AlGaInP LEDs with a conventional quarter-wave DBR (b) Schematics of the vertical radiation through the top surface.

As seen in Fig. 1(a), the transparent p-doped GaP layer (~8 μm) occupies most of the wave guiding structure. Therefore, the horizontal radiation through four side facets is also significant (Fig. 2(b)). The horizontal radiation increases as the transparent GaP layer becomes thicker because the horizontal radiation experiences smaller internal absorption losses before it escapes out of the device [12]. Therefore it will be advantageous if one finds a DBR structure that reports minimal absorption losses for both types of radiation.

3. Solid angle optimization for vertical radiation

As mentioned previously, the conventional quarter-wave DBR shows maximum reflectance at a normal angle. This design principle works well for vertical-cavity surface-emitting lasers and does not guarantee the maximum extraction for LEDs. In the AlGaInP material system, the radiation of an LED is assumed to be isotropic and shows no preferred direction. Therefore, with the center wavelength fixed at 625 nm, one needs to find the optimum reflectance angle (θ_M) of the DBR that maximizes the flux through the top hemisphere.

To find out the optimal θ_M, the normalized angle integrated reflectivity (R_v) is defined as shown in Eq. (1) and the resultant R_v is plotted in the Fig. 3(a). Here, $I(\lambda)$ is the spectral intensity of the AlGaInP MQWs and θ_c is the critical angle for the top interface. $R_{\theta M}(\theta, \lambda)$ is the reflectance at the corresponding incident angle and radiation wavelength when the maximum reflectance angle equals to θ_M. Here, the ambient medium is assumed to be epoxy (n=1.4).

$$R_v(\theta_M) = \int_0^{\theta_c} R_{\theta_M}(\theta,\lambda) I(\lambda) Sin\theta \, d\theta \, d\lambda \,/\, R_v(\theta_M = 0^\circ) \qquad (1)$$

#92654 - $15.00 USD Received 11 Feb 2008; revised 9 Apr 2008; accepted 9 Apr 2008; published 14 Apr 2008

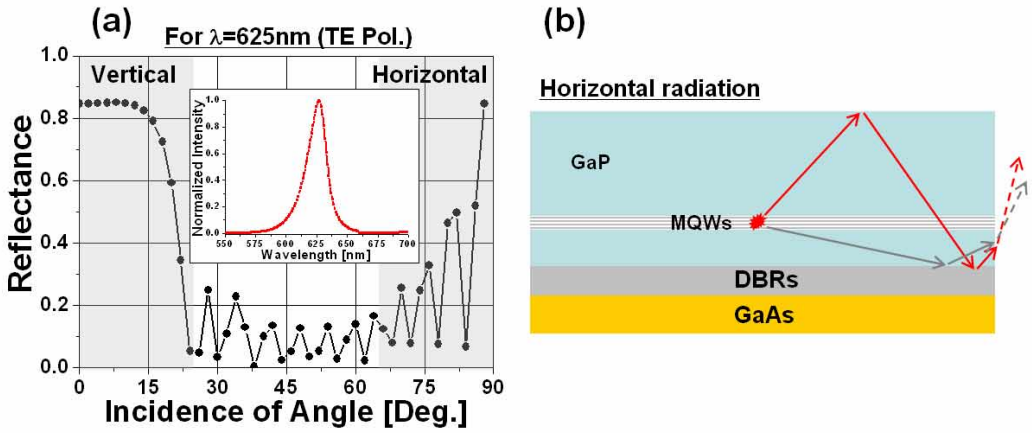

Fig. 2. (a) Angular reflectance of the conventional DBR. The inset shows a typical spectrum of the AlGaInP LED. (b) Schematics of the horizontal radiation through four side facets.

The maximum R_v is found when θ_M=17.5°, which is about two third of the critical angle. The angular reflectance plots for the conventional and optimized DBRs are shown in the inset of Fig. 3 (a). Obviously, the increase of the normalized vertical reflectivity from the optimized DBRs is attributed to the fact that the oblique angle radiation occupies larger solid angle.

4. Evanescent decoupling for horizontal radiation

As represented in Fig. 2(a), the reflectance of the conventional DBR is generally low when the incident angle is between 70~90°. This low reflectance results from the small index contrast between an incident medium (AlInP, n=3.32) and the low index layer (AlAs, n=3.13). If the AlAs layer is sufficiently thick, then the evanescent coupling is discouraged and the total internal reflection at AlInP/AlAs interface becomes dominant for an incident angle beyond the critical angle (70.5°). However, the TIRs are easily frustrated through photon tunneling when the attenuation length of the evanescent field is comparable to the thickness of the lower index medium [8].

In our modified DBR, the total pairs of the DBRs are 12.5, just adding a half period to the conventional DBRs. The thickness of the first low index layer (t_{L1}) is designed thicker than the attenuation length to decouple the evanescent field. The thickness of the other layers (t') is angle-tuned to maximize the vertical radiation, as aforementioned. Fig. 3(b) shows the reflectance spectra at the incident angle of 75° for various t_{L1} values. Note that this angle is clearly beyond the critical angle at the AlInP/AlAs interface. The reflectance reaches unity when t_{L1}=7t'. For the incident angle steeper than 75°, the TIR effect undoubtedly becomes more significant because the evanescent field range is shorter. Note that the reflectivity for the vertical radiation is almost unchanged by modifying the thickness of the first AlAs layer as long as it equals to odd multiples of a quarter wave.

In fact, the design principle of the modified DBRs consisting of low index top layer is same as the internal omni-directional reflector described in Ref. [8]. But, the difference is our internal omni-directional reflector use epitaxial layer so that the electrical characteristic of the device is not degraded. Furthermore, our reflector is monolithically fabricated without additional deposition processes.

#92654 - $15.00 USD Received 11 Feb 2008; revised 9 Apr 2008; accepted 9 Apr 2008; published 14 Apr 2008

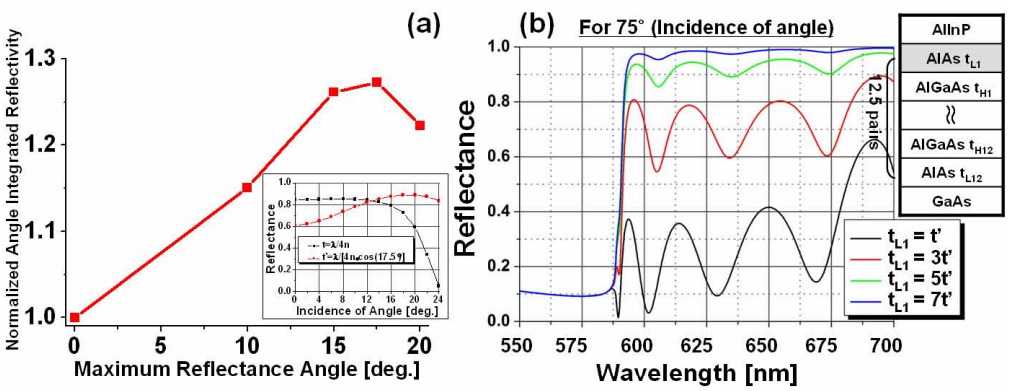

Fig. 3. (a) The normalized angle integrated reflectivity (R_v) versus the maximum reflectance angle (θ_M). The inset shows the angular reflectance for the conventional- and improved DBRs (θ_M=17.5°) at the center wavelength (λ=625nm). (b) Reflectance spectrum varying the first AlAs layer (t_{L1}) thickness

5. Demonstration of the improved DBRs

In order to verify the performance of our proposed design, we prepare AlGaInP LEDs with the conventional- and improved DBRs. To avoid other issues affecting the output power, both DBRs are grown under the identical epitaxial growth environment (Fig. 1(a)). The only difference is the thickness of each DBR layer. Fig. 4(a) shows the cross sections of DBRs captured by a transmission electron microscope (TEM). One can see that the first AlAs layer is seven times thicker than the other layer.

The AlGaInP LEDs are fabricated by following standard fabrication steps. A backside n-ohmic electrode composed of AuGe/Ni/Au (120, 30, 300 nm) is deposited by an e-beam evaporation process. Subsequently, the top p-ohmic electrode composed of AuBe/Au (150, 500 nm) is formed by an electron beam evaporation process and typical photolithography lift-off, in turn. The total emitting area is 1.1x1.1 mm^2. The final processed LED devices are mounted *p*-side-up on a lead frame and then encapsulated with dome-shaped epoxy (n=1.4). All the subsequent measurements are carried out using a conventional integration sphere.

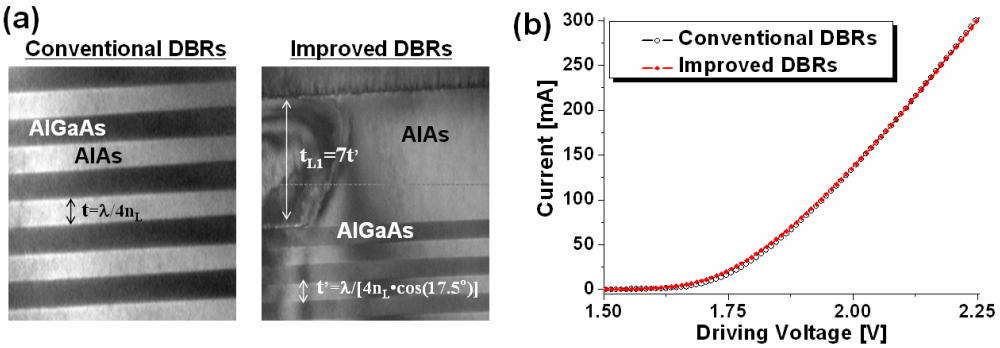

Fig. 4. (a) Cross section TEM image of the conventional- and improved DBRs (b) I-V characteristic curves for the devices with both DBRs

First, we compare I-V (current-voltage) characteristics to examine whether the modification of thickness in the improved DBRs affects their electrical properties (Fig. 4(b)). Apparently, no degradation is observed on the I-V curve. Next, the output power before and

#92654 - $15.00 USD Received 11 Feb 2008; revised 9 Apr 2008; accepted 9 Apr 2008; published 14 Apr 2008

after encapsulation is recorded as the injected current is swept up to 500 mA (Fig. 5(a)). The integration sphere measurement covers the whole emission spectrum of the AlGaInP LEDs (λ_c=625 nm, $\Delta\lambda$=18 nm). At a standard current of 350 mA, the integrated output power of the optimized DBRs after encapsulation is enhanced by factor of ~1.9 in comparison to the conventional DBRs. The enhancement before encapsulation at the same current is somewhat smaller (~1.8 fold), because the improved DBR is optimally designed for epoxy (n=1.4). In addition, it is interesting to observe that the relative output enhancement is larger at low current [Fig. 5(a)]. For the AlGaInP MQWs, the drop of the internal radiative efficiency due to device heating at higher current results in reduction of the output enhancement [5]. Since the horizontal radiation passes through the MQWs several times before the escape, it is heavily influenced by their absorption. Therefore, the higher relative enhancement at low current is ascribed to the horizontal radiation that experiences the more transparent active medium. Note that the peak emission wavelength is changed with the current. However, the shift of wavelength (~4nm) while the current sweeping from 10 to 500 mA barely affects the vertical reflectivity of the DBRs. Lastly, we compare the radiation profiles of two structures [Fig. 5(b)]. The width of the angular distribution of the optimized DBRs is somewhat larger than that of the conventional DBRs. This observation also supports our claim that the horizontal radiation of the optimized DBRs contributes to the total radiation.

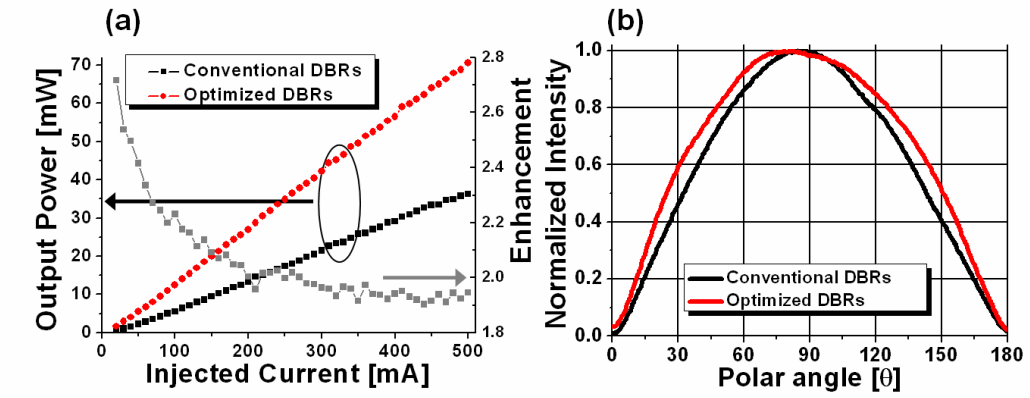

Fig. 5. (a) L-I (light-current) curve for the devices with both DBRs. The output enhancement versus the injected current is also plotted. (b) Measurement of the angular radiation profile for the devices with both DBRs (before encapsulation)

6. Incorporation of two-dimensional photonic crystal

Although we implemented modified DBRs in LEDs, many photons are still trapped by TIRs. In order to further improve the extraction efficiency, it is essential to incorporate additional light extraction structures to overcome TIRs. Randomly roughened surfaces [9] and the periodic photonic crystal [10-11] are commonly employed to defeat the total internal reflection. The roughened surface is usually textured by a proper chemical etchant. This simple process is sometimes disadvantageous in realizing a structure with optimum pit density and size. On the contrary, the periodic pattern has better degrees of design freedom that can be implemented. For instance, lattice constant, filling-factor, and etch depth can be adjusted separately to realize a specific pattern.

Experimentally, we introduce two-dimensional square-lattice photonic crystal into the top p-GaP surface. A broad range of lattice constant has shown extraction enhancement with increase of etch depth [13-15]. It is also known that deeply-etched holes interact strongly with higher-order guided modes. The optimal lattice constant can be often extended up to a-few-wavelengths (>>λ/n).

Conventional photolithography (h-line, λ_p=405nm) techniques are employed to define the periodic holes (Fig. 6(a)). The lattice constant and the hole diameter are 1200 nm and 800 nm,

#92654 - $15.00 USD Received 11 Feb 2008; revised 9 Apr 2008; accepted 9 Apr 2008; published 14 Apr 2008

respectively. These structural parameters are well within the resolution of the photolithography. To create the etch mask, a SiO_2 thin film layer is deposited by a sputtering process before the periodic pattern is defined onto it. The SiO_2 thin film and p-doped GaP surface are etched using inductively coupled plasma reactive ion etching with $Ar/CHF_3/CF_4$ and $Ar/BCl_3/Cl_2$, respectively. The etch depth of the p-doped GaP surface is made as deep as 1.0 μm to extract higher-order guided modes effectively when the lattice constant is 1200 nm. After the patterning processes of AlGaInP LEDs (1.1x1.1 mm^2) with the optimized DBR, the n- and p-electrode are formed by the same procedure. .

Fig. 6(b) compares the integrated output power with a reference (flat surface) and the photonic crystal. Additional enhancement of ~25% is achieved at a standard current of 350 mA. We would like to emphasize that this lattice distance (1200nm) can be realized even through the conventional photolithography.

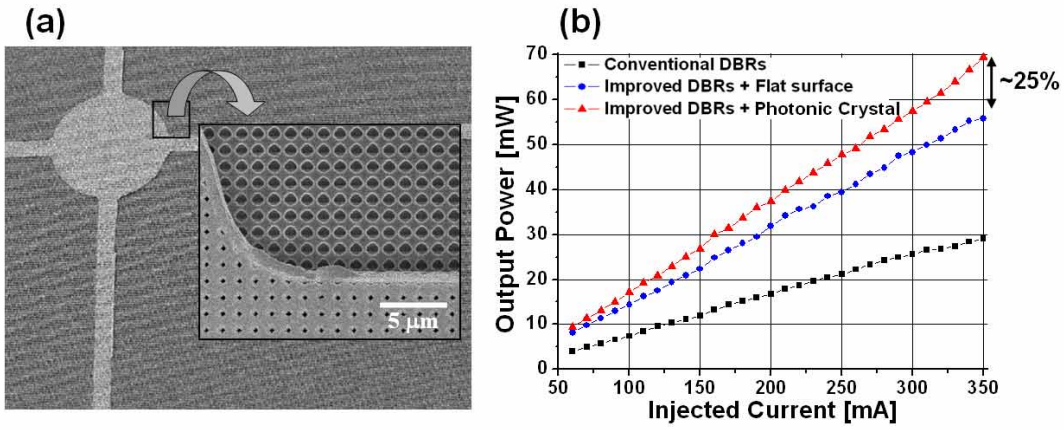

Fig. 6. (a) Scanning electron microscope image of the periodic pattern defined into the top p-GaP surface (b) L-I curves for devices with conventional DBRs, the optimized DBRs with flat surface and the optimized DBRs with two-dimensional photonic crystal.

7. Summary

We demonstrate two explicit ways to improve the extraction efficiency of the AlGaInP LED. First, the AlAs/AlGaAs DBR is optimized to enhance the radiation through vertical- and horizontal pathways. The thickness of each DBR layer is enlarged by 1/cos17.5° to maximize the normalized vertical reflectivity accumulated within a critical angle of the top interface. Then, the first lower index layer (AlAs) is made seven times thicker than the other layers to prevent evanescent coupling losses for enhanced horizontal radiation. The integration sphere measurement shows relative output enhancement of ~1.9-fold in comparison to the LED with conventional DBRs. Second, we incorporate square lattice periodic holes (a=1200 nm) into the top GaP surface by a conventional photolithography (λ_p=405 nm). The output enhancement of ~1.25-fold is additionally observed in comparison with the LEDs with flat surfaces. It is remarkable that this micron-scale periodic pattern can be manufactured by the low-cost and high-throughput lithography fabrication techniques.

#92654 - $15.00 USD Received 11 Feb 2008; revised 9 Apr 2008; accepted 9 Apr 2008; published 14 Apr 2008